

# Site-selectivity of 3d metal cation dopants and dielectric response in calcium copper titanate

Sung-Yoon Chung<sup>a)</sup>

*Department of Materials Science and Engineering, Inha University, Incheon 402-751, Korea*

Si-Young Choi

*Institute of Engineering Innovation, The University of Tokyo, Tokyo 113-8656, Japan*

Takahisa Yamamoto

*Department of Advanced Materials Science, The University of Tokyo, Tokyo 113-8656, Japan*

Yuichi Ikuhara

*Institute of Engineering Innovation, The University of Tokyo, Tokyo 113-8656, Japan*

Suk-Joong L. Kang

*Department of Materials Science and Engineering, Korea Advanced Institute of Science and Technology, Daejeon 305-701, Korea*

(Received 31 October 2005; accepted 13 January 2006; published online 2 March 2006)

By doping a few atomic percent of 3d-block cations, we demonstrate that the high dielectric response in  $\text{CaCu}_3\text{Ti}_4\text{O}_{12}$  can be reduced by a factor of  $\sim 10^3$  at room temperature. Each of the added dopants shows its own preferential substitution on either Cu or Ti sites. The dopants that act as acceptors have a critical impact on the disappearance of the electrostatic potential barrier at grain boundaries, resulting in drastically decreased permittivity values of  $< 90$  without voltage dependence. The present doping experiment directly shows that the potential barrier at internal interfaces is a key factor for the peculiar dielectric phenomena. © 2006 American Institute of Physics. [DOI: 10.1063/1.2179110]

Since the first report in 2000 on the gigantic permittivity and unusual dielectric behaviors of  $\text{CaCu}_3\text{Ti}_4\text{O}_{12}$  (CCTO),<sup>1</sup> a number of studies have focused on this titanate over the last 5 years with a remarkable surge of interest.<sup>2–15</sup> The dielectric characteristics that have been recognized in CCTO include very high permittivity values of  $\sim 10^5$  without any ferroelectric or relaxor-type phase transition in a wide range of temperature.<sup>1,2</sup> In addition, such high dielectric constants drastically decrease to less than 100 below 80 K, with no accompanying change in the crystal structure as the temperature varies.<sup>1–3</sup>

Earlier researches on CCTO suggested that intrinsic local dipole moments induced by the Ti displacement could be responsible for the high permittivity,<sup>1–3</sup> as in other high-dielectric titanates. The first-principles calculations, on the other hand, have indicated that the lattice has a marginal intrinsic contribution to the dielectric response,<sup>4,6</sup> giving possible explanations based on extrinsic effects.<sup>8</sup> An analysis using impedance spectroscopy<sup>5</sup> has for the first time experimentally shown that polycrystalline CCTO consists of conducting regions and insulating layers, similar to those in internal barrier-layer capacitors. In particular, recent studies have demonstrated that an electrostatic potential barrier exists at grain boundaries,<sup>9,14</sup> supporting the electrically inhomogeneous microstructure. Although researchers now seem to accept that extrinsic factors have an effect on the enormous permittivity, no direct experimental evidence has been provided to demystify the peculiar dielectric phenomena in CCTO.

By adding various 3d metal cations as dopants, this study shows that each dopant has its own preferred substitu-

tional site when incorporated into the CCTO lattice. We also demonstrate that certain dopants have a critical influence on the extinction of an electrical barrier at grain boundaries and a reduction in the number of charge carriers in bulk grains as well. Furthermore, we observe that the value of dielectric permittivity decreases by three orders of magnitude, reaching a value as low as  $\sim 80$ , when the electrostatic potential at grain boundaries disappears through selective doping. The correlation between the electrical barrier at internal interfaces and the giant dielectric behavior of CCTO is discussed on the basis of this experimental evidence.

Doped CCTO powder was synthesized using high-purity  $\text{CaCO}_3$ ,  $\text{CuO}$ ,  $\text{TiO}_2$ ,  $\text{NiO}$ ,  $\text{CoO}$ ,  $\text{Cr}_2\text{O}_3$ , and  $\text{Fe}_2\text{O}_3$ . The starting composition of the powders is  $\text{CaCu}_3(\text{Ti}_{4-x}\text{M}_x)\text{O}_{12}$ , where  $M$  is  $\text{Cr}^{3+}$ ,  $\text{Fe}^{3+}$ ,  $\text{Co}^{2+}$ , or  $\text{Ni}^{2+}$ , and  $x$ , the added amount of each dopant, is 0.2 (5 at. % on Ti sites). Experimental procedures for the preparation of densified compacts are the same in the previous reports.<sup>9,15</sup> X-ray diffraction (Rigaku DMAX-2500) was used for phase identification after crushing dense pellets sintered at 1100 °C in air for 20 h. We used a microprobe station (The Micromanipulator) and tungsten probes (2  $\mu\text{m}$  in diameter) to measure the current-voltage ( $I$ - $V$ ) across individual grain boundaries and within single crystalline grains. Densely sintered pellets were also used for the  $I$ - $V$  measurements (Model 237, Keithley). The capacitances (HP 4192A) using the same pellets were measured as a function of applied voltage from  $-20$  V to  $+20$  V at 100 kHz with an oscillation voltage of 1 V. Grains with more than 20  $\mu\text{m}$  in diameter were selected in each of the well-polished dense pellets for quantitative electron probe microanalysis (EPMA-1600, Shimadzu). We used an undoped pellet as a standard crystal for quantification of Ca, Cu, and Ti. The size of the electron probe was 5  $\mu\text{m}$  at an

<sup>a)</sup>Electronic mail: sychung@inha.ac.kr

TABLE I. Quantitative comparison of concentration ratios between cations within grains by electron probe microanalysis.<sup>a</sup>

(%)	Ca/(Ca+Cu+Ti+M)	Cu/(Ca+Cu+Ti+M)	Ti/(Ca+Cu+Ti+M)	M/(Ca+Cu+Ti+M)
Undoped ( <i>M</i> =0)				
Theoretical values	12.5	37.5	50.0	...
Co-doped	12.2±0.1	35.2±0.2	49.9±0.2	2.72±0.01
Ni-doped	12.3±0.3	34.7±0.3	50.3±0.3	2.78±0.05
Fe-doped	12.2±0.2	37.1±0.5	48.0±0.4	2.72±0.10
Cr-doped	12.2±0.2	37.4±0.4	47.8±0.3	2.65±0.08

<sup>a</sup>*M*=Co, Ni, Fe, Cr.

accelerating voltage of 15 keV and a beam current of 20 nA.

From the x-ray diffractometry (not shown here), an additional CuO phase could be identified in both the Co- and Ni-doped specimens, while there was no detectable secondary phase in the Cr- and Fe-doped specimens. Considering the initial formula of the starting materials, the presence of a secondary CuO phase implies that the added Co and Ni ions are substituted for Cu rather than for Ti. To make a quantitative investigation on the concentration change among the cations inside the bulk grains, we carried out an electron probe microanalysis (EPMA) using well-polished dense pellets that were  $\sim 20 \mu\text{m}$  in grain size. More than 20 grains were examined in each specimen so as to obtain accurate statistics. Table I summarizes the average concentration ratios and the standard deviation between cations including the dopant. The specimens containing Co and Ni clearly show Cu deficiency compared to the reference concentration ratio of an undoped specimen, while Ti is observed to be deficient for both Cr- and Fe-doped specimens. Therefore, in accordance with the x-ray diffraction, the EPMA result provides direct evidence that most of the added Co and Ni are preferentially substituted for Cu, whereas Cr and Fe occupy the Ti site in CCTO.

*I-V* behaviors were measured across individual grain boundaries as well as within single crystalline grains. Figure 1(a) shows the *I-V* relationship of an undoped specimen. Consistent with the previous result,<sup>9</sup> the current flow across a grain boundary (between electrodes 3 and 4) is observed to be suppressed due to an electrostatic potential barrier at grain boundaries, in contrast to the measurement within a grain between electrodes 1 and 2. When Co is doped, *I-V* variations similar to those observed in the undoped specimen can be measured [Fig. 1(b)], because Co and Ni in the same valence state as Cu basically have no influence on the electronic properties of the CCTO lattice.

Fe and Cr on Ti sites, on the other hand, had an enormous impact on the *I-V* characteristics. First, it is noted that the amount of current flowing within a grain is drastically reduced, by a factor of  $10^3$ , from a microampere to a nanoampere scale, as shown in Fig. 1(c). Furthermore, the *I-V* behaviors are almost identical to each other over the measurements between electrodes, indicating that essentially no electrostatic barrier is present at the grain boundaries. A previous study<sup>9</sup> suggested that the electron energy band structure across the grain boundary in undoped CCTO is equivalent to *n-i-n* based on the *n*-type semiconducting grains with a conductivity of  $\sim 10^{-3} \text{ S/cm}$  and the interface traps for electrons at the boundary region, although the origin of the intrinsic donor defects responsible for the *n*-type grains re-

mains unidentified. Since the added Cr and Fe act as acceptors, the unknown donor defects in the lattice are no longer compensated by electrons. Instead they are compensated mainly by these acceptor ions, resulting in a reduction in the number of free electrons within the grains. This leads to a negligible difference in the Fermi energy level between a grain and a grain boundary and, consequently, to virtually no bending in the electron energy band structure at the boundary regions.

Figure 2 shows the plots of the current density (*J*) versus the electric field (*E*) for doped and undoped CCTO sintered

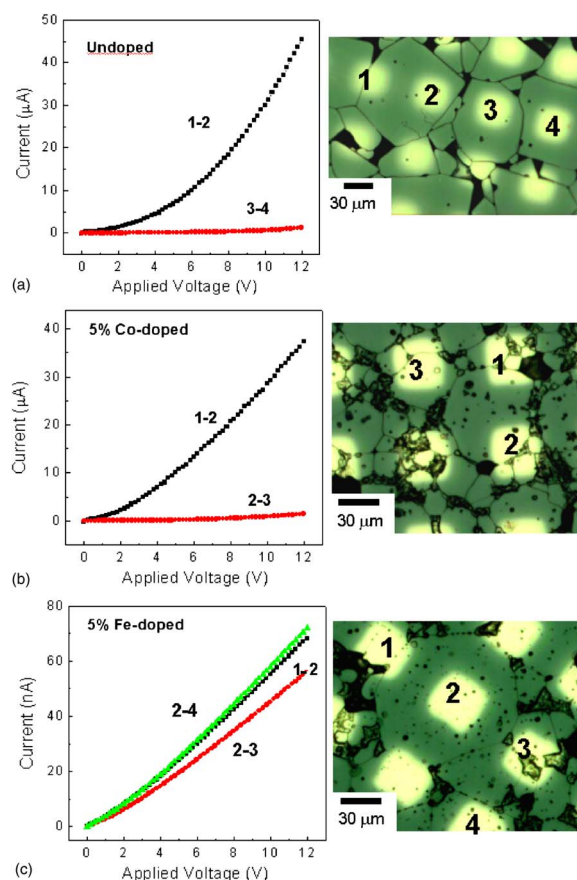


FIG. 1. (Color online) *I-V* characteristics and surface morphologies with gold microelectrodes. Each electrode is numbered for reference. (a) Undoped pure specimen. (b) 5 at. % Co-doped specimen. *I-V* behavior similar to that in the undoped specimen is shown. These *I-V* characteristics were also found for Ni doping. (c) 5 at. % Fe-doped specimen. Note the scale of the current in the plot. The overall current flows are drastically reduced, and no difference in *I-V* characteristics is exhibited between electrodes. The 5 at. % Cr-doped specimen displayed identical characteristics.

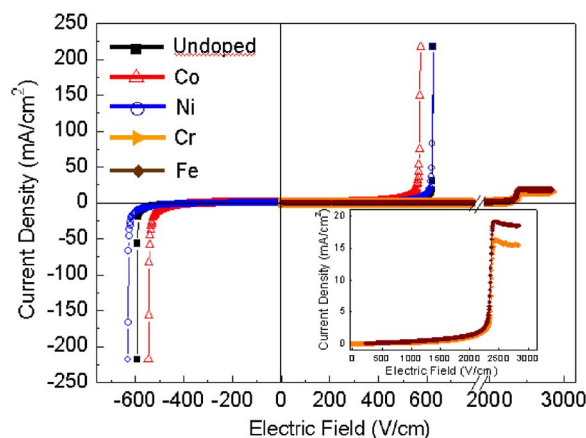


FIG. 2. (Color online) Current density-electric field ( $J$ - $E$ ) characteristics of pellets sintered at  $1100^\circ\text{C}$  in air for 20 h. The inset shows that both the Cr- and Fe-doped samples dielectrically break down at around 2300 V/cm.

at  $1100^\circ\text{C}$  in air for 20 h. As shown in the figure, the same nonlinear  $I$ - $V$  characteristics as in the undoped specimen are observed in both Co and Ni doped specimens. However, the Cr- and Fe-doped specimens show no abrupt change in current density as the applied field varies. The inset of Fig. 2 indicates that a dielectric breakdown occurs around 2300 V/cm, as in typical dielectrics. Along with the above microscale  $I$ - $V$  measurements, the low current density over the whole range of applied bias demonstrates that the acceptor-type Cr and Fe ions at the Ti site are responsible for the electrical homogeneity without electrostatic barriers at the grain boundaries.

We also measured the variation of capacitance ( $C$ ) as a function of applied bias ( $V$ ) for each specimen in order to investigate the effect of dopants on the dielectric property. Figure 3 presents the plots of apparent permittivity against applied voltage at 100 kHz. Compared with other ferroelectric materials, undoped CCTO exhibits very different  $C$ - $V$  behavior. Its permittivity linearly varies with applied voltage without hysteresis, as plotted in Fig. 3(a). Co- and Ni-doped specimens also show the same linear characteristics in their  $C$ - $V$  curves [Figs. 3(b) and 3(c)]. Because both dopants are substituted for only 5% of the Cu sites without forming any charged defects, the absence of a critical difference between undoped, Co-, and Ni-doped CCTO in terms of dielectric properties is not surprising. In contrast, doping of the Cr and Fe ions affects the dielectric response considerably. The most notable change upon doping Cr and Fe is that the permittivity value decreases by three orders of magnitude, reaching  $\sim 88$ , as shown in Figs. 3(d) and 3(e). The linear variation of the voltage-dependent permittivity observed in the undoped specimen also disappears, and the permittivity remains almost constant irrespective of the magnitude of applied voltage.

In summary, the present experimental results for 3d metal cation-doped specimens clearly demonstrate the close relationship between the giant dielectric phenomenon and the electrostatic potential barrier at internal interfaces in CCTO. Doping with only a few atomic percent of acceptors efficiently removes the potential barrier by reducing the free electron density in bulk grains, and thus makes a specimen electrically homogeneous. This significant decrease in the value of the dielectric constant for the case of acceptor dop-

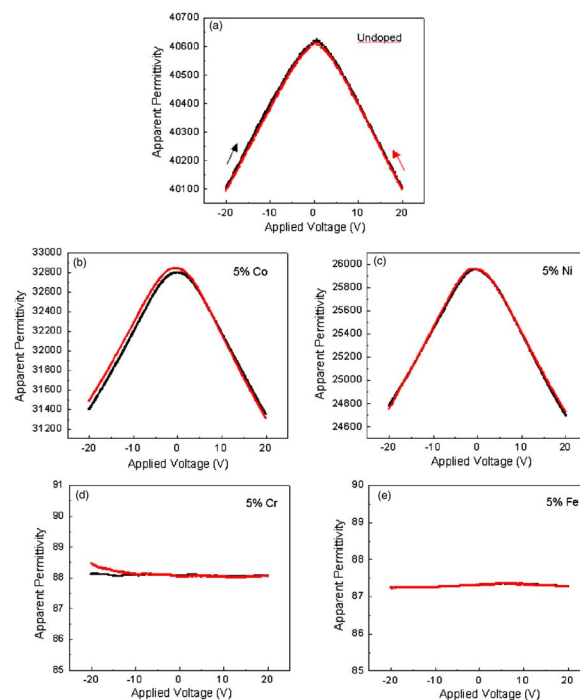


FIG. 3. (Color online) Variations of apparent permittivity with applied voltage. Plots of (a) undoped, (b) 5 at. % Co-, (c) 5 at. % Ni-, (d) 5 at. % Cr-, and (e) 5 at. % Fe-doped specimen sintered at  $1100^\circ\text{C}$  in air for 20 h are shown. Note that the permittivity has been reduced by three orders of magnitude in (d) and (e).

ing indicates that the apparent high dielectric response of CCTO is attributed to the semiconducting grains and insulating internal interfaces that act as a thin dielectric layer. For detailed information related to the potential barrier at grain boundaries, analytical investigations are ongoing.

The authors thank Y. B. Lee at the Korea Basic Science Institute (KBSI) in Jeonju for assistance with EPMA. This research was supported by the Korea Research Foundation (KRF), Grant No. R05-2004-000-10168-0.

- <sup>1</sup>M. A. Subramanian, D. Li, N. Duan, B. A. Reisner, and A. W. Sleight, *J. Solid State Chem.* **151**, 323 (2000).
- <sup>2</sup>A. P. Ramirez, M. A. Subramanian, M. Gardel, G. Blumberg, D. Li, T. Vogt, and S. M. Shapiro, *Solid State Commun.* **115**, 217 (2000).
- <sup>3</sup>C. C. Homes, T. Vogt, S. M. Shapiro, S. Wakimoto, and A. P. Ramirez, *Science* **293**, 673 (2001).
- <sup>4</sup>L. He, J. B. Neaton, M. H. Cohen, D. Vanderbilt, and C. C. Homes, *Phys. Rev. B* **65**, 214112 (2002).
- <sup>5</sup>D. C. Sinclair, T. B. Adams, F. D. Morrison, and A. R. West, *Appl. Phys. Lett.* **80**, 2153 (2002).
- <sup>6</sup>L. He, J. B. Neaton, D. Vanderbilt, and M. H. Cohen, *Phys. Rev. B* **67**, 012103 (2003).
- <sup>7</sup>C. C. Homes, T. Vogt, S. M. Shapiro, S. Wakimoto, M. A. Subramanian, and A. P. Ramirez, *Phys. Rev. B* **67**, 092106 (2003).
- <sup>8</sup>M. H. Cohen, J. B. Neaton, L. He, and D. Vanderbilt, *J. Appl. Phys.* **94**, 3299 (2003).
- <sup>9</sup>S.-Y. Chung, I.-D. Kim, and S.-J. L. Kang, *Nat. Mater.* **3**, 774 (2004).
- <sup>10</sup>L. Zhang and Z.-J. Tang, *Phys. Rev. B* **70**, 174306 (2004).
- <sup>11</sup>G. Chiodelli, V. Massarotti, D. Capsoni, M. Bini, C. B. Azzoni, M. C. Mozzati, and P. Lupotto, *Solid State Commun.* **132**, 241 (2004).
- <sup>12</sup>R. K. Grubbs, E. L. Venturini, P. G. Clem, J. J. Richardson, B. A. Tuttle, and G. A. Samara, *Phys. Rev. B* **72**, 104111 (2005).
- <sup>13</sup>L. Wu, Y. Zhu, S. Park, S. Shapiro, G. Shirane, and J. Taftø, *Phys. Rev. B* **71**, 014118 (2005).
- <sup>14</sup>S. V. Kalinin, J. Shin, G. M. Veith, A. P. Baddorf, M. V. Lobanov, H. Runge, and M. Greenblatt, *Appl. Phys. Lett.* **86**, 102902 (2005).
- <sup>15</sup>S.-Y. Chung, *Appl. Phys. Lett.* **87**, 052901 (2005).